NIH Public Access
Author Manuscript
Gastroenterology. Author manuscript; available in PMC 2012 October 1.

Published in final edited form as:
Gastroenterology. 2011 October ; 141(4): 1463–1472. doi:10.1053/j.gastro.2011.06.045.

Extensive Pancreas Regeneration Following Acinar-Specific Disruption of Xbp1 in Mice

David A. Hess[*,1], **Sean E. Humphrey**[*,1], **Jeff Ishibashi**[1], **Barbara Damsz**[1], **Ann-Hwee Lee**[2], **Laurie H. Glimcher**[2], and **Stephen F. Konieczny**[+,1]

[1]Department of Biological Sciences and the Purdue Center for Cancer Research, Purdue University, West Lafayette, IN 47907

[2]Department of Immunology and Infectious Diseases, Harvard School of Public Health and Department of Medicine, Harvard Medical School, Boston, MA 02115

Abstract

Background & Aims—Progression of diseases of the exocrine pancreas, which include pancreatitis and cancer, is associated with increased levels of cell stress. Pancreatic acinar cells are involved in development of these diseases and, because of their high level of protein output, they require an efficient, unfolded protein response (UPR), which mediates recovery from endoplasmic reticulum (ER) stress following the accumulation of misfolded proteins.

Methods—To study recovery from ER stress in the exocrine organ, we generated mice with conditional disruption of *Xbp1* (a principle component of the UPR) in most adult pancreatic acinar cells ($Xbp1^{fl/fl}$). We monitored the effects of constitutive ER stress in the exocrine pancreas of these mice.

Results—Xbp1-null acinar cells underwent extensive apoptosis, followed by a rapid phase of recovery in the pancreas that included expansion of the centroacinar cell compartment, formation of tubular complexes that contained Hes1- and Sox9-expressing cells, and regeneration of acinar cells that expressed Mist1 from the residual, surviving Xbp1+ cell population.

Conclusions—XBP1 appears to be required for homeostatisis of acinar cells in mice; ER stress induces a regenerative response in the pancreas that involves acinar and centroacinar cells and promotes organ recovery from exocrine pancreas disease.

Keywords

endoplasmic reticulum stress; pancreatic progenitor cells; protein folding; tissue regeneration

© 2011 The American Gastroenterological Association. Published by Elsevier Inc. All rights reserved.

[+]**Corresponding Author:** Department of Biological Sciences and the Purdue Center for Cancer Research Purdue University Hansen Life Sciences Research Building 201 South University Street West Lafayette, IN 47907-2064 Tel: 765-494-7976 sfk@purdue.edu .
[*]these authors contributed equally to this work.

Author Contributions: DAH, SEH, BD designed and performed experiments; JI assisted in interpretation of data; AHL, LHG provided reagents and critically evaluated data; SFK designed and analyzed experiments; DAH, SFK wrote the manuscript.

Publisher's Disclaimer: This is a PDF file of an unedited manuscript that has been accepted for publication. As a service to our customers we are providing this early version of the manuscript. The manuscript will undergo copyediting, typesetting, and review of the resulting proof before it is published in its final citable form. Please note that during the production process errors may be discovered which could affect the content, and all legal disclaimers that apply to the journal pertain.

Disclosure Statement: The authors have no disclosures to report.

NIH-PA Author Manuscript
NIH-PA Author Manuscript
NIH-PA Author Manuscript

NIH-PA Author Manuscript

NIH-PA Author Manuscript

NIH-PA Author Manuscript

Introduction

The pancreas is a complex secretory organ tasked with endocrine-mediated maintenance of blood glucose levels and exocrine production of key enzymatic components of the digestive system. Defects or damage to various pancreatic cells contribute to multiple disease states including diabetes, pancreatitis and pancreatic cancer, the latter two being diseases associated with the exocrine pancreas. An understanding of the response of pancreatic tissues to damage and stress is of great interest as a means of exploring the development of disease and as a potential avenue for therapeutic intervention.

As professional secretory cells, pancreatic acinar cells are responsible for the synthesis, storage and secretion of vast quantities of digestive hydrolases that assist in food digestion [1]. One of the key requirements for the proper function and survival of acinar cells is the management of their extensive protein synthesis/processing machinery that utilizes regulatory pathways involving the Golgi, intermediate transport vesicles, plasma membrane components and the endoplasmic reticulum (ER). Among these organelles, the ER insures that newly synthesized secretory and transmembrane proteins are properly folded and modified prior to exportation. In cells with high protein synthesis demands [2, 3], specific differentiation requirements [2, 4, 5], or that are subject to environmental or physiological alterations, the ability of the protein-folding machinery to handle the current demands of newly synthesized proteins can reach an imbalance, setting in motion a series of intracellular signaling pathways collectively known as the unfolded protein response (UPR) [6, 7, 8]. Activation of the UPR allows cells to adjust to high protein demands by transcriptionally activating genes that increase protein-folding capacity.

The UPR consists of three distinct signaling arms (IRE1/XBP1, ATF6, PERK), each of which activates unique downstream target genes and pathways (*e.g.*, XBP1 - PDI, Sec61a; ATF6 - nATF6α; PERK - p-eIF2α) [8]. The ER inositol-requiring transmembrane kinase/endonuclease 1 (IRE1) branch activates multiple classes of molecules including chaperones (PDI), protein transporters (Sec61a) and growth/DNA damage regulators (GADD153/CHOP). IRE1 oligomerizes and autophosphorylates in response to unfolded proteins in the ER lumen, resulting in activation of its novel endoribonuclease domain. Activated IRE1 excises a 26 nt fragment within the basal Xbp1 transcript, producing a frame shift and consequent translation of a 371 a.a. XBP1s ("spliced") transcription factor that functions to upregulate UPR target genes [2, 8].

The high protein synthesis capacity of pancreatic acinar cells suggests that they likely rely on an efficient IRE1/XBP1 pathway to maintain proper protein processing [9]. In support of this idea, Iwawaki et al. have shown that the IRE1/XBP1 pathway is constitutively active in the exocrine pancreas [10, 11]. Similarly, acinar cells undergoing acute pancreatitis exhibit elevated levels of ER stress accompanied by activation of the Xbp1 splicing machinery [6, 7, 10]. Indeed, embryonic deletion in $Xbp1^{-/-}$;Liv^{XBP1} mice results in pancreata that are severely devoid of acinar cells, leading to neonatal death due to limited food digestion and consequent hypoglycemia [3]. XBP1 is also essential for plasma cell differentiation [2] and is critical for tumor angiogenesis in pancreatic adenocarcinoma [11], revealing a central role for this factor in many different biological contexts. Since XBP1 possesses additional functions in normal cell development [2, 4, 12] outside of ER stress maintenance, it has been difficult to assess the importance of the IRE1/XBP1 pathway in the adult exocrine pancreas. To circumvent this obstacle, we conditionally inactivated an $Xbp1^{fl/fl}$ allele in adult acinar cells to address two key questions: (a) what is the fate of individual acinar cells undergoing chronic ER stress in the absence of the IRE1/XBP1 pathway; and (b) how does the exocrine organ cope with defective secretory cells? Our results demonstrate that loss of XBP1 function is lethal to mature acinar cells. However, the

NIH-PA Author Manuscript

NIH-PA Author Manuscript

NIH-PA Author Manuscript

pancreas itself exhibits a remarkable ability to recover from chronic ER stress by eliciting a rapid regeneration response from a minority of unrecombined $Xbp1^{fl/fl}$ acinar cells as well as from Hes1/Sox9 positive centroacinar progenitor cells. We conclude that the IRE1/XBP1 pathway is critical to maintaining normal ER homeostasis and that exploiting ER stress represents a novel approach to generating and studying pancreatic damage *in vivo*.

Materials and Methods

Mouse strains and genotyping

$Mist1^{CreER/+}$ and $Xbp1^{fl/fl}$ mice have been described previously [4, 13, 14]. Induction of $Cre-ER^{T2}$ activity was accomplished by providing adult mice (6-8 wk) tamoxifen (4 mg/mouse/day) for 2 consecutive days. Mice were sacrificed at 1 week intervals following tamoxifen addition and pancreata were harvested using standard protocols. Genotyping and recombination primer sets are listed in Supplemental Table I. All studies were conducted in compliance with NIH and the Purdue University IACUC guidelines.

Histology and immunohistochemistry

Mouse pancreata were fixed in 10% neutral buffered formalin, paraffin embedded, sectioned to 5 μM and stained using conventional hematoxylin and eosin. Sections were deparaffinized and retrieved using the 2100-Retriever (PickCell Laboratories, Amsterdam, The Netherlands) and antigen unmasking solution (Vector Laboratories). Samples were blocked using the MOM blocking reagent (Vector Laboratories) and incubation of primary antibodies was conducted overnight at 4°C. Biotinylated secondary antibodies were applied for 10 min at 25°C. Visualization was accomplished via DAB peroxidase staining (Vector Labs) or tertiary, avidin-conjugated fluorescent antibodies. Primary antibodies and conditions are provided in Supplemental Table II. TUNEL assays were performed following digestion in 250 μg/mL proteinase K in 2.5 mmol/L $CaCl_2$, 10 mmol/L Tris-HCl, pH 7.5 for 1 min at 25°C using the in situ death detection kit (Roche, Indianapolis, IN).

Electron microscopy

Pancreata were fragmented and fixed in 3% paraformaldehyde-0.5% gluteraldehyde in PBS, then gradually dehydrated and embedded in epon resin. Electron micrographs were obtained from ultrathin sections using a Philips transmission electron microscope.

Protein immunoblot assays

20 μg of whole cell protein extracts were separated on 12% acrylamide gels, transferred to PVDF membranes and incubated with primary antibodies (antibody conditions are provided in Supplemental Table III). Immunoblots were developed using an ECL kit (Pierce, Rockford, IL).

RT-qPCR gene expression analysis

Pancreas RNA was isolated using the RNeasy isolation system (QIAGEN, Valencia, CA) and reverse transcribed using the iScript™ cDNA synthesis kit (Bio-Rad, Hercules, CA). cDNA reactions were amplified with QPCR SYBR Green Mix (ABgene) as described in Supplemental Methods using the primer sets listed in Supplemental Table IV.

Results

Acinar-restricted deletion of Xbp1

To examine the importance of XBP1 and the UPR pathway to the mature exocrine pancreas we utilized conditional null $Xbp1^{fl/fl}$ mice [4] crossed to $Mist1^{CreER/+}$ mice which express

NIH-PA Author Manuscript

NIH-PA Author Manuscript

NIH-PA Author Manuscript

CreER^{T2} exclusively in acinar cells [13, 14] (Figure 1A). Control pancreata from vehicle-treated adult Xbp1$^{fl/fl}$; Mist1$^{CreER/+}$ mice showed no signs of Cre-mediated recombination and were phenotypically indistinguishable from pancreata obtained from wild type, Xbp1$^{fl/fl}$ or Mist1$^{CreER/+}$ animals (Figure 1B, S1). In contrast, tamoxifen (TM)-treated Xbp1$^{fl/fl}$; Mist1$^{CreER/+}$ mice exhibited pancreas-restricted recombination that deleted exon 2 from the Xbp1 locus (Figure 1B). As predicted, TM administration also led to pancreas-specific expression of Xbp1$^{\Delta Ex2}$ transcripts within 24 hr (Figure 1C). Lineage tracing using Xbp1$^{fl/fl}$; Mist1$^{CreER/+}$; R26^{LacZ} mice revealed no recombination in the absence of TM but robust recombination (β-gal+, blue) in approximately 90% of acinar cells (Figure 1D,E).

To establish the importance of XBP1 to adult acinar cell homeostasis, we next analyzed individual Xbp1$^{fl/fl}$; Mist1$^{CreER/+}$ (+TM) animals (hereafter named Xbp1$^{\Delta Ex2}$) over an extended time course. As expected, mice heterozygous for Xbp1 (Xbp1$^{\Delta Ex2/+}$) exhibited no signs of ER stress (Figure S1). In contrast, Xbp1$^{\Delta Ex2}$ pancreata showed large increases in the general ER stress pathway components Bip and Chop as well as within the PERK and ATF6 arms of the UPR as indicated by increased levels of phospho-eIF2α and nuclear ATF6α, the immediate effectors of PERK and ATF6, respectively (Figure 2A) (see Supplemental Table V for a list of individual molecular markers used in this study). Similarly, the XBP1 arm of the UPR exhibited elevated expression of Xbp1s transcripts over this period (Figure 2B). However, since Xbp1s$^{\Delta Ex2}$ transcripts generate a nonfunctional protein [4], normal XBP1 downstream target genes including Sec61a and PDI were not significantly induced (Figure 2B). Examination of acinar cell differentiation markers revealed a 60-70% reduction in amylase and elastase levels over the duration of the study (Figure 2C,D). Likewise, the 37 kD cleaved, active form of carboxypeptidase A (CPA^{Active}) was readily detected in Xbp1$^{\Delta Ex2}$ pancreata, reflecting an induced damage response since pancreas CPA is normally stored as an inactive proenzyme except in cases of injury (Figure 2D) [15]. Therefore, loss of Xbp1 results in significant alterations in acinar cell properties despite activation of the remnant UPR pathways.

Even with large changes in the expression profiles of UPR pathway components and acinar cell differentiation genes, Xbp1$^{\Delta Ex2}$ pancreata at 24 hr or 1 wk post-TM had no significant gross morphology deficiencies. Early time point Xbp1$^{\Delta Ex2}$ acinar cells exhibited the typical accumulation of zymogen granules (ZG) and normal apical-basal organization of functional acini (Figure 3A). However, by 2 wk post-TM, Xbp1$^{\Delta Ex2}$ pancreata showed substantial alterations in acinar cell structure, with a reduction in ZG and loss of cytoplasmic area (Figure 3B). At 4 wk, Xbp1$^{\Delta Ex2}$ pancreata were severely compromised. Ducts and islets were grossly normal (Figure S2) while the vast majority of acinar cells were defective, showing a complete loss of ZG accumulation and a greatly reduced cytoplasmic footprint (Figure 3C). These changes were vividly illustrated by transmission electron microscopy. Low magnification examination of toluidine-stained semi-thin sections from 4 wk post-TM samples revealed extensive disruption of the exocrine pancreas where the vast majority of acinar cells had greatly reduced cytoplasm and only rare ZG (Figure 3D). The few ZG in Xbp1$^{\Delta Ex2}$ acinar cells were small and lacked electron dense material, or were found within autophagic complexes (Figure 3E,F; S3). Analysis of ER architecture revealed a poorly developed and dilated ER with disorganized cisternae within Xbp1$^{\Delta Ex2}$ acinar cells. This was in contrast to the elaborately organized and densely packed ER found in control acinar cells. Whereas the majority of ribosomes in control pancreata were ER-associated, Xbp1$^{\Delta Ex2}$ acinar cells were filled with abundant free ribosomes that were not part of the defective ER (Figure 3E,F; S3). Taken together, these results demonstrate that, in the absence of functional XBP1 protein, the exocrine pancreas undergoes a sustained period of ER stress.

NIH-PA Author Manuscript

NIH-PA Author Manuscript

NIH-PA Author Manuscript

Xbp1$^{\Delta Ex2}$ pancreata exhibit two distinct acinar cell populations

Although most of the Xbp1$^{\Delta Ex2}$ exocrine pancreas consisted of a non-zymogenic acinar cell population 4 wk following recombination of the Xbp1$^{fl/fl}$ locus, small isolated clusters of relatively normal (zymogenic) acinar cells remained within the organ (Figure 3C,D). These cells retained a typical acinus structure and contained large numbers of ZGs, suggesting that they represented the ~10% acinar cells that failed to undergo Cre-mediated recombination of the Xbp1$^{fl/fl}$ locus (see Figure 1D,E). Indeed, lineage tracing on 4 wk Xbp1$^{\Delta Ex2}$; R26^{LacZ} mice revealed that the non-zymogenic acinar cell population were almost entirely β-gal+, identifying those cells as Xbp1$^{\Delta Ex2}$ cells (Figure 4A, S4). In contrast, isolated groups of intact, zymogenic-acinar cells remained mostly β-gal−, although rare (~1%) β-gal+ zymogenic cells were observed, presumably reflecting cells that successfully recombined the R26^{LacZ} locus but not both Xbp1$^{fl/fl}$ alleles. As predicted, the β-gal negative acinar cell units maintained high levels of amylase expression (Figure 4B). The zymogenic cells also expressed nuclear MIST1 protein (Figure 4B), which is required to maintain key acinar cell properties [15]. Xbp1$^{\Delta Ex2}$ pancreata exhibited a 3.5-fold increase in overall Mist1 transcript levels despite having only ~10% of cells expressing MIST1 protein (Figure 4C). In contrast, β-gal+, non-zymogenic cells barely retained detectable levels of acinar cell markers (Figure 4B). The non-zymogenic cells also had elevated levels of specific ER stress pathway components - for instance, 98% of all CHOP+ cells were non-zymogenic cells (Figure 4D). Cells expressing CHOP were also prone to apoptosis, as TUNEL staining revealed a dramatic increase in the number of apoptotic cells over the 4 wk post-TM period with the majority (96%) found within the non-zymogenic, β-gal+ cell population (Figure 4D). These cells also exhibited autophagy and activation of other stress pathway components including elevated levels of pErk1/2 and p38 as part of their terminal endpoint response to loss of XBP1 (Figure S5), confirming a critical role for XBP1 in controlling cellular homeostasis.

The extensive tissue damage that occurred over the 4 wk post-TM period in Xbp1$^{\Delta Ex2}$ pancreata prompted us to ask if the organ responded to loss of XBP1 by activating transcription programs associated with pancreatic progenitor cells during embryonic development or pancreatic injury. Previous studies have shown that pancreatic progenitor cells increase expression of a number of genes including Nestin and the transcription factors Hes1 and Sox9, proteins normally restricted to centroacinar cells [16-19]. Each of these genes is up-regulated in the Xbp1$^{\Delta Ex2}$ model, with maximum expression detected at 4 wk (Figure 4E). Expression of both proteins was restricted to centroacinar/terminal duct cells in the Xbp1$^{\Delta Ex2}$ pancreata (Figure 4F). Zymogenic and non-zymogenic cells remained Hes1/Sox9 negative. Thus, extensive Xbp1$^{\Delta Ex2}$-induced apoptosis leads to a massive damage response within the exocrine pancreas that includes activation of putative Hes1/Sox9 pancreas progenitor cells.

Xbp1$^{\Delta Ex2}$ pancreata initiate a potent regeneration response to replace the acinar cell compartment

Although approximately 90% of the Xbp1$^{\Delta Ex2}$ exocrine pancreas was severely disrupted in 4 wk post-TM mice (see Figure 3C,D), dramatic changes in pancreas gene expression patterns occurred over the ensuing 2 wk. Expression of downstream ER stress pathway genes, including Bip, Chop, p-eIF2α, nATGF6α and Xbp1u → Xbp1s splicing quickly returned to control basal levels by 6 wk post-TM (Figure 5A). Similarly, Nestin, Hes1 and Sox9 transcripts peaked at 4 wk post-TM and then returned to near control levels by 6 wk (Figure 5B). Changes in differentiation genes were also observed with Mist1 transcripts peaking at 4 wk post-TM but gradually returning to control levels by 6 wk (Figure 5C). The decreases in Mist1, Nestin, Hes1 and Sox9 transcripts correlated with a resurgence in Amylase and Elastase transcripts and disappearance of cleaved (active) CPA, such that

NIH-PA Author Manuscript

NIH-PA Author Manuscript

NIH-PA Author Manuscript

expression of zymogen hydrolases returned to control levels by 6 wk post-TM (Figure 5D,E).

The complete restoration of molecular markers to control levels after 6 wk suggested that the apoptotic $Xbp1^{\Delta Ex2}$ acinar cells were replaced, possibly from the small subset that escaped TM-induced recombination. By 4 wk post-TM the remaining $Xbp1^{fl/fl}$ zymogenic cells were generally present as individual acinus units scattered among the apoptotic, non-zymogenic population. These β-gal negative cells showed a dramatic increase in cell proliferation that peaked at 6 wk post-TM (Figure 6A, S6). Indeed, greater than 80% of all proliferating cells at this time point were zymogenic acinar cells with the remaining proliferative cells mostly Sox9 positive centroacinar/terminal duct cells (Figure 6B). Additionally, the regeneration response also included transient up-regulation of the Reg1 gene (Figure S6). As predicted, despite extensive β-gal expression from the $R26^{LacZ}$ locus in 4 wk samples, few β-gal+ cells remained at the later time points, and this decrease correlated with a loss of $Xbp1^{\Delta Ex2}$ transcripts as $Xbp1^{\Delta Ex2}$ acinar cells were replaced by $Xbp1^{fl/fl}$ acinar cells (Figure 6C,D, S7).

Morphometry analysis of 6-8 wk post-TM pancreata revealed an almost complete recovery from the $Xbp1^{\Delta Ex2}$ phenotype. The exocrine pancreas consisted predominantly of zymogen-filled acini with little evidence of apoptotic cells (Figure 6E). Although there was a significant increase in adipose tissue, most of the exocrine organ consisted of relatively normal appearing acinar cells (Figure 6F). However, intermixed with acini were limited areas that retained inflammatory cells, as well as extensive Sox9 positive tubular complexes which were likely derived from the proliferating Hes1/Sox9 positive centroacinar/terminal duct cell population (Figure 6F, S8).

Finally, we examined 8-12 wk $Xbp1^{\Delta Ex2}$ pancreata to determine if regenerated acinar cells resembled age-matched control pancreata. Regenerated acinar cells had well-defined acini that were filled with ZG (Figure 7A,B). However, individual acinar cells at 8 wk post-TM were significantly larger than control $Xbp1^{fl/fl}$ cells (Figures 7B,C). Zymogenic cell volumes increased steadily from 2-6 wk post-TM after which the regenerating acinar cells were almost 2.5-fold larger than control cells. Interestingly, zymogenic cell nuclei also showed an increase in volume, attaining sizes that were 3-fold larger than normal acinar nuclei (Figure 7D). By 12 wk post-TM, acinar nuclear and cell size remained approximately 2-fold larger than control litter mate samples. These results suggest that regenerated cells exhibited a hypertrophic response, possibly as a resilient mechanism to cope with the extensive cell death associated with $Xbp1^{\Delta Ex2}$ cells.

Discussion

Understanding the molecular pathways by which cells, tissues and organs respond and recover from stress is critical to accurately predict and appropriately intercede when aberrant physiological responses present. Cellular coping mechanisms are often driven by specific responses to a pertinent stressor, including the three pathways collectively termed the unfolded protein response (UPR). The UPR is an important homeostatic mechanism in all cells, but its function is especially important for secretory cells utilizing high throughput translational machinery. In this study, we conditionally inactivated the Xbp1 locus in adult acinar cells to establish the importance of the XBP1 component of the UPR to exocrine pancreas physiology. Our results support a direct and essential role for XBP1 in modulating ER stress events and in maintaining viability of adult acinar cells.

Acinar-specific ablation of Xbp1 triggered a rapid ER stress response within 24 hr with the PERK, ATF6 and IRE/XBP1 pathways activated, but Xbp1-specific downstream targets

NIH-PA Author Manuscript

NIH-PA Author Manuscript

NIH-PA Author Manuscript

uninduced. Despite an otherwise intact UPR, Xbp1$^{\Delta Ex2}$ adult acinar cells were chronically under ER stress, revealing for the first time that the PERK and ATF6 pathways are insufficient for recovery from ER stress in these cells. The inability of acinar cells to compensate for loss of XBP1 was surprising, given reports that acinar-restricted deletion of PERK failed to produce ER stress [20]. Similarly, germ-line deletion of ATF6α resulted in no cellular or organ defects, although ATF6α$^{-/-}$ MEFs were more susceptible to chemically-induced ER stress [21]. Together, these results support the concept that IRE/XBP1 is the major UPR pathway utilized by acinar cells to maintain proper ER homeostasis.

Deletion of Xbp1 in a number of specialized secretory cells, including plasma B cells and intestinal Paneth cells, induces significant ER stress and associated alterations in ER architecture [2, 22, 23]. A similar outcome has recently been observed in stomach zymogenic cells (ZCs) where deletion of Xbp1 induced ER stress and an altered ER. However, unlike pancreatic acinar cells, Xbp1$^{\Delta Ex2}$ stomach ZCs survived without this critical regulator, with no evidence of cell loss following Xbp1 deletion [12]. Indeed, stomach ZCs arising after Xbp1 ablation continued to express zymogenic cell markers, although defects in the developmental silencing of progenitor neck cell markers were observed [12]. This is in marked contrast to pancreatic acinar cells which rapidly lose differentiated cell markers and increase expression of CHOP, a known inducer of apoptosis via repression of Bcl-2. The dramatic difference in cell viability between stomach ZCs and pancreatic acinar cells suggests that the PERK and ATF6 pathways are utilized to different extents in these functionally related cell types. Additional studies will be required to determine how the distinct arms of the UPR function during development and in mature adult cells within different secretory cell lineages.

Despite extensive cell death throughout the Xbp1$^{\Delta Ex2}$ exocrine pancreas, isolated areas of zymogen-containing acinar cells remained, representing the small portion of cells that failed to ablate Xbp1. Interestingly, the escaping Xbp1$^{fl/fl}$ acinar cells no longer remained quiescent but quickly entered a proliferative phase, a response that is similarly observed in caerulein injury models of regeneration [24-26]. The Xbp1$^{fl/fl}$ zymogenic acinar cells also retained high levels of MIST1 protein, indicating that these cells failed to completely abrogate their terminal exocrine differentiation program during the proliferative phase. This contrasts with caerulein injury and Kras^{G12D}-induced acinar-ductal metaplasia, where MIST1 levels are quickly extinguished during the early phases of injury and dedifferentiation [27]. Thus, depending on the initial insult, acinar cells may be capable of utilizing different recovery pathways to regenerate.

In addition to acinar cell regeneration, deletion of Xbp1 in acinar cells also led to proliferation of the centroacinar and terminal duct cell population, distinguishable by expression of the transcription factors Sox9 and Hes1 [16-19]. Elegant studies by Rovira et al. have shown that this cell population is capable of forming self-renewing pancreatospheres that spontaneously give rise to cells of the endocrine and acinar cell lineages *in vitro* [16]. This population also becomes greatly expanded in the setting of caerulein-induced pancreatitis [16], suggesting that a similar regeneration phenomenon occurs upon acinar-specific deletion of Xbp1. Although lineage tracing studies can not be performed on the centroacinar/terminal duct cells in this current Xbp1$^{fl/fl}$ model, these cells are likely responsible for formation of the Sox9/K19 expressing tubular complexes that form in the recovered pancreas [18, 19]. Additional studies will be required to define the fate of the expanded centroacinar cell compartment and to determine if these cells also contribute to other cell lineages upon chronic ER stress.

The coordinate pancreatic regeneration observed in this model is accompanied by an acquisition of the normal exocrine pancreas parameters of zymogen production and

NIH-PA Author Manuscript

NIH-PA Author Manuscript

NIH-PA Author Manuscript

activation, expression of hallmark transcription factors including Mist1, and a marked reduction in proliferation markers. These changes indicate that the regenerated acinar cells begin to re-establish proper pancreatic function following the elimination of the CHOP+, Xbp1-deficient population. Indeed, acini in the recovering organ have a marked increase in cell size, presumably due to compensatory overproduction of zymogens in these acini as the pancreas continues to regenerate. Thus, our study demonstrates that pancreatic renewal can occur, despite a severe ER stress-induced apoptotic event, via proliferation and compensation of the surviving exocrine compartment.

Finally, the regenerative capacity of the adult pancreas in the presence of an ER stress-based alteration provides a unique opportunity to exploit UPR pathways for therapeutic purposes. Studies utilizing modification of the UPR to compromise transformed cell growth have shown promise in cancer cell lines [28] and in murine models of tumor development [29], and several studies have shown efficacy of bortezomib in sensitizing pancreatic cancer cells to ER stress induced apoptosis [30-32]. Future approaches should focus on (a) developing new cell targeted strategies to inhibit XBP1 function in pancreatic tumors and (b) increasing the regenerative response of the remaining nontransformed cells of the exocrine pancreas.

Supplementary Material

Refer to Web version on PubMed Central for supplementary material.

Acknowledgments

We thank Dr. Michael Logan for providing histopathology analysis, David Miley for generating histology slides and Patrick Schweickert for quantitative analysis.

Grant Support: This work was supported by grants to SFK (NIH DK55489, CA124586), LHG (NIH AI32412) and AHL (AHA 0835610P).

Abbreviations

ATF6	activating transcription factor-6
β-gal	β-galactosidase
CHOP	C/EBP-homologous protein
CPA	carboxypeptidase
Cre-ER	Cre recombinase-estrogen receptor
ER	endoplasmic reticulum
IRE	inositol-requiring transmembrane kinase/endonuclease 1
K19	keratin 19
pH3	phospho-histone 3
PERK	protein kinase RNA-like ER kinase
PDI	protein disulfide isomerase
Sec61a	subunit of the Sec61 transport protein complex
TM	tamoxifen
TUNEL	terminal deoxynucleotidyl transferase dUTP nick end labeling
UPR	unfolded protein response

NIH-PA Author Manuscript

NIH-PA Author Manuscript

NIH-PA Author Manuscript

Xbp1	X-box binding protein 1
Xbp1s	Xbp1 spliced version
Xbp1$^{fl/fl}$	floxed Xbp1 allele
Xbp1$^{\Delta Ex2}$	Xbp1 exon 2 deleted version
ZG	zymogen granule

References

1. Williams JA. Regulation of acinar cell function in the pancreas. Curr Opin Gastroenterol. 2010; 26:478–83. [PubMed: 20625287]
2. Todd DJ, McHeyzer-Williams LJ, Kowal C, Lee AH, Volpe BT, Diamond B, McHeyzer-Williams MG, Glimcher LH. XBP1 governs late events in plasma cell differentiation and is not required for antigen-specific memory B cell development. J Exp Med. 2009; 206:2151–9. [PubMed: 19752183]
3. Lee AH, Chu GC, Iwakoshi NN, Glimcher LH. XBP-1 is required for biogenesis of cellular secretory machinery of exocrine glands. Embo J. 2005; 24:4368–80. [PubMed: 16362047]
4. Lee AH, Scapa EF, Cohen DE, Glimcher LH. Regulation of hepatic lipogenesis by the transcription factor XBP1. Science. 2008; 320:1492–6. [PubMed: 18556558]
5. Back SH, Scheuner D, Han J, Song B, Ribick M, Wang J, Gildersleeve RD, Pennathur S, Kaufman RJ. Translation attenuation through eIF2alpha phosphorylation prevents oxidative stress and maintains the differentiated state in beta cells. Cell Metab. 2009; 10:13–26. [PubMed: 19583950]
6. Kowalik AS, Johnson CL, Chadi SA, Weston JY, Fazio EN, Pin CL. Mice lacking the transcription factor Mist1 exhibit an altered stress response and increased sensitivity to caerulein-induced pancreatitis. Am J Physiol Gastrointest Liver Physiol. 2007; 292:G1123–32. [PubMed: 17170023]
7. Kubisch CH, Logsdon CD. Secretagogues differentially activate endoplasmic reticulum stress responses in pancreatic acinar cells. Am J Physiol Gastrointest Liver Physiol. 2007; 292:G1804–12. [PubMed: 17431218]
8. Ron D, Walter P. Signal integration in the endoplasmic reticulum unfolded protein response. Nat Rev Mol Cell Biol. 2007; 8:519–29. [PubMed: 17565364]
9. Kubisch CH, Logsdon CD. Endoplasmic reticulum stress and the pancreatic acinar cell. Expert Rev Gastroenterol Hepatol. 2008; 2:249–60. [PubMed: 19072360]
10. Kubisch CH, Sans MD, Arumugam T, Ernst SA, Williams JA, Logsdon CD. Early activation of endoplasmic reticulum stress is associated with arginine-induced acute pancreatitis. Am J Physiol Gastrointest Liver Physiol. 2006; 291:G238–45. [PubMed: 16574987]
11. Romero-Ramirez L, Cao H, Regalado MP, Kambham N, Siemann D, Kim JJ, Le QT, Koong AC. X box-binding protein 1 regulates angiogenesis in human pancreatic adenocarcinomas. Transl Oncol. 2009; 2:31–8. [PubMed: 19252749]
12. Huh WJ, Esen E, Geahlen JH, Bredemeyer AJ, Lee AH, Shi G, Konieczny SF, Glimcher LH, Mills JC. XBP1 controls maturation of gastric zymogenic cells by induction of MIST1 and expansion of the rough endoplasmic reticulum. Gastroenterology. 2010; 139:2038–49. [PubMed: 20816838]
13. Habbe N, Shi G, Meguid RA, Fendrich V, Esni F, Chen H, Feldmann G, Stoffers DA, Konieczny SF, Leach SD, Maitra A. Spontaneous induction of murine pancreatic intraepithelial neoplasia (mPanIN) by acinar cell targeting of oncogenic Kras in adult mice. Proc Natl Acad Sci U S A. 2008; 105:18913–8. [PubMed: 19028870]
14. Shi G, Zhu L, Sun Y, Bettencourt R, Damsz B, Hruban RH, Konieczny SF. Loss of the acinar-restricted transcription factor Mist1 accelerates Kras-induced pancreatic intraepithelial neoplasia. Gastroenterology. 2009; 136:1368–78. [PubMed: 19249398]
15. Pin CL, Rukstalis JM, Johnson C, Konieczny SF. The bHLH transcription factor Mist1 is required to maintain exocrine pancreas cell organization and acinar cell identity. J Cell Biol. 2001; 155:519–30. [PubMed: 11696558]

NIH-PA Author Manuscript

NIH-PA Author Manuscript

NIH-PA Author Manuscript

16. Rovira M, Scott SG, Liss AS, Jensen J, Thayer SP, Leach SD. Isolation and characterization of centroacinar/terminal ductal progenitor cells in adult mouse pancreas. Proc Natl Acad Sci U S A. 2010; 107:75–80. [PubMed: 20018761]

17. Seymour PA, Freude KK, Tran MN, Mayes EE, Jensen J, Kist R, Scherer G, Sander M. SOX9 is required for maintenance of the pancreatic progenitor cell pool. Proc Natl Acad Sci U S A. 2007; 104:1865–70. [PubMed: 17267606]

18. Furuyama K, Kawaguchi Y, Akiyama H, Horiguchi M, Kodama S, Kuhara T, Hosokawa S, Elbahrawy A, Soeda T, Koizumi M, Masui T, Kawaguchi M, Takaori K, Doi R, Nishi E, Kakinoki R, Deng JM, Behringer RR, Nakamura T, Uemoto S. Continuous cell supply from a Sox9-expressing progenitor zone in adult liver, exocrine pancreas and intestine. Nat Genet. 2011; 43:34–41. [PubMed: 21113154]

19. Kopinke D, Brailsford M, Shea JE, Leavitt R, Scaife CL, Murtaugh LC. Lineage tracing reveals the dynamic contribution of Hes1+ cells to the developing and adult pancreas. Development. 2011; 138:431–41. [PubMed: 21205788]

20. Iida K, Li Y, McGrath BC, Frank A, Cavener DR. PERK eIF2 alpha kinase is required to regulate the viability of the exocrine pancreas in mice. BMC Cell Biol. 2007; 8:38. [PubMed: 17727724]

21. Wu J, Rutkowski DT, Dubois M, Swathirajan J, Saunders T, Wang J, Song B, Yau GD, Kaufman RJ. ATF6alpha optimizes long-term endoplasmic reticulum function to protect cells from chronic stress. Dev Cell. 2007; 13:351–64. [PubMed: 17765679]

22. Reimold AM, Iwakoshi NN, Manis J, Vallabhajosyula P, Szomolanyi-Tsuda E, Gravallese EM, Friend D, Grusby MJ, Alt F, Glimcher LH. Plasma cell differentiation requires the transcription factor XBP-1. Nature. 2001; 412:300–7. [PubMed: 11460154]

23. Kaser A, Lee AH, Franke A, Glickman JN, Zeissig S, Tilg H, Nieuwenhuis EE, Higgins DE, Schreiber S, Glimcher LH, Blumberg RS. XBP1 Links ER Stress to Intestinal Inflammation and Confers Genetic Risk for Human Inflammatory Bowel Disease. Cell. 2008; 134:743–56. [PubMed: 18775308]

24. Desai BM, Oliver-Krasinski J, De Leon DD, Farzad C, Hong N, Leach SD, Stoffers DA. Preexisting pancreatic acinar cells contribute to acinar cell, but not islet beta cell, regeneration. J Clin Invest. 2007; 117:971–7. [PubMed: 17404620]

25. Fendrich V, Esni F, Garay MV, Feldmann G, Habbe N, Jensen JN, Dor Y, Stoffers D, Jensen J, Leach SD, Maitra A. Hedgehog signaling is required for effective regeneration of exocrine pancreas. Gastroenterology. 2008; 135:621–31. [PubMed: 18515092]

26. Strobel O, Dor Y, Alsina J, Stirman A, Lauwers G, Trainor A, Castillo CF, Warshaw AL, Thayer SP. In vivo lineage tracing defines the role of acinar-to-ductal transdifferentiation in inflammatory ductal metaplasia. Gastroenterology. 2007; 133:1999–2009. [PubMed: 18054571]

27. Jensen JN, Cameron E, Garay MV, Starkey TW, Gianani R, Jensen J. Recapitulation of elements of embryonic development in adult mouse pancreatic regeneration. Gastroenterology. 2005; 128:728–41. [PubMed: 15765408]

28. Romero-Ramirez L, Cao H, Nelson D, Hammond E, Lee AH, Yoshida H, Mori K, Glimcher LH, Denko NC, Giaccia AJ, Le QT, Koong AC. XBP1 is essential for survival under hypoxic conditions and is required for tumor growth. Cancer Res. 2004; 64:5943–7. [PubMed: 15342372]

29. Bobrovnikova-Marjon E, Grigoriadou C, Pytel D, Zhang F, Ye J, Koumenis C, Cavener D, Diehl JA. PERK promotes cancer cell proliferation and tumor growth by limiting oxidative DNA damage. Oncogene. 2010; 29:3881–95. [PubMed: 20453876]

30. Nawrocki ST, Carew JS, Dunner K Jr. Boise LH, Chiao PJ, Huang P, Abbruzzese JL, McConkey DJ. Bortezomib inhibits PKR-like endoplasmic reticulum (ER) kinase and induces apoptosis via ER stress in human pancreatic cancer cells. Cancer Res. 2005; 65:11510–9. [PubMed: 16357160]

31. Nawrocki ST, Carew JS, Pino MS, Highshaw RA, Andtbacka RH, Dunner K Jr. Pal A, Bornmann WG, Chiao PJ, Huang P, Xiong H, Abbruzzese JL, McConkey DJ. Aggresome disruption: a novel strategy to enhance bortezomib-induced apoptosis in pancreatic cancer cells. Cancer Res. 2006; 66:3773–81. [PubMed: 16585204]

32. Nawrocki ST, Carew JS, Pino MS, Highshaw RA, Dunner K Jr. Huang P, Abbruzzese JL, McConkey DJ. Bortezomib sensitizes pancreatic cancer cells to endoplasmic reticulum stress-mediated apoptosis. Cancer Res. 2005; 65:11658–66. [PubMed: 16357177]

NIH-PA Author Manuscript

NIH-PA Author Manuscript

NIH-PA Author Manuscript

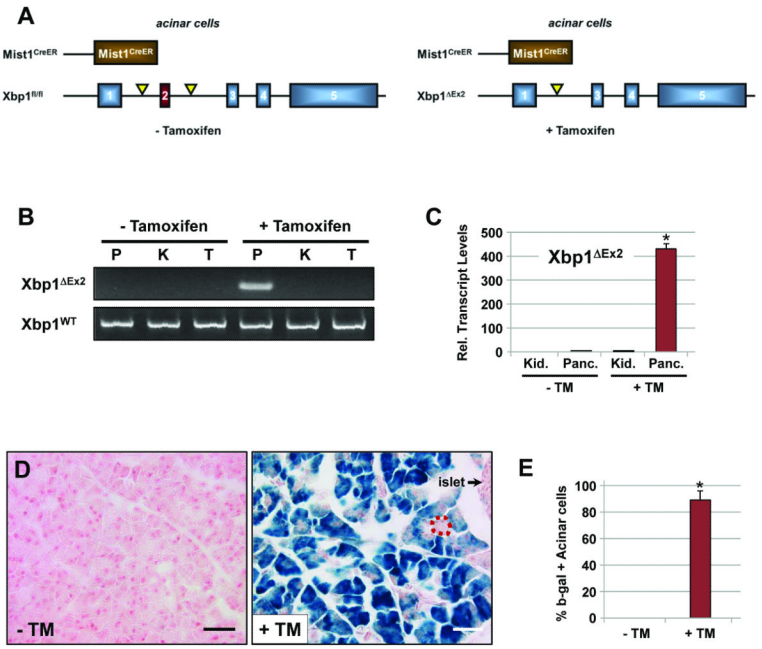

Figure 1. Xbp1$^{fl/fl}$;Mist1$^{CreER/+}$ mice selectively ablate Xbp1 in pancreatic acinar cells

(A) Schematic representation of the Xbp1$^{fl/fl}$ and Xbp1$^{\Delta Ex2}$ alleles from untreated and tamoxifen-treated mice. **(B)** Xbp1$^{\Delta Ex2}$-specific PCR reveals pancreas-restricted excision of exon 2 following TM treatment (P - pancreas, K - kidney, T - tail DNA). **(C)** Transcript analysis of the recombined Xbp1$^{\Delta Ex2}$ locus confirms Xbp1$^{\Delta Ex2}$ transcripts exclusively in pancreatic samples post-TM (Kid. - kidney, Panc. - pancreas RNA). **(D)** Representative fields of Xbp1$^{fl/fl}$;Mist1$^{CreER/+}$;R26R^{LacZ} pancreata treated with or without TM and stained for β-galactosidase (β-gal). Dotted red outline shows a rare β-gal negative acinus. Scale = 40 μm. **(E)** Quantification of β-gal positive acinar cells in Xbp1$^{fl/fl}$;Mist1$^{CreER/+}$;R26R pancreata. *p<0.005

NIH-PA Author Manuscript

NIH-PA Author Manuscript

NIH-PA Author Manuscript

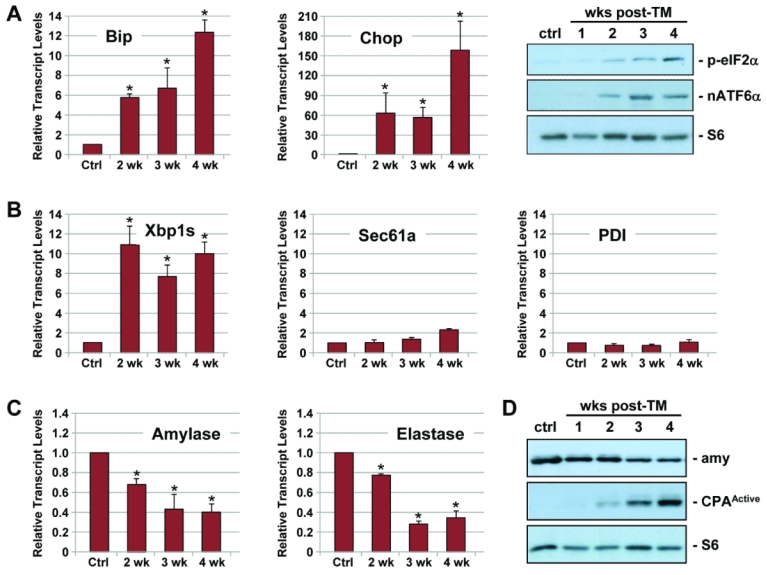

Figure 2. Activation of the UPR following acinar-specific ablation of Xbp1

(A) Relative transcript or protein levels of common ER stress indicators including BiP, Chop, phospho-eIF2α and nuclear ATF6α and **(B)** Xbp1s following ablation of Xbp1 over the indicated post-TM time points. **(B)** Xbp1-specific targets Sec61a and PDI do not exhibit increased expression following Xbp1 ablation. **(C)** Relative transcript levels of amylase and elastase are decreased following Xbp1 ablation. **(D)** Protein blots revealing decreased production of amylase and increased production of the cleaved, active form of carboxypeptidase (CPA^{Active}), an indicator of intracellular damage to acinar cells. Anti-S6 - loading control. Ctrl - litter mate animals treated with corn oil. *$p<0.05$

NIH-PA Author Manuscript
NIH-PA Author Manuscript
NIH-PA Author Manuscript

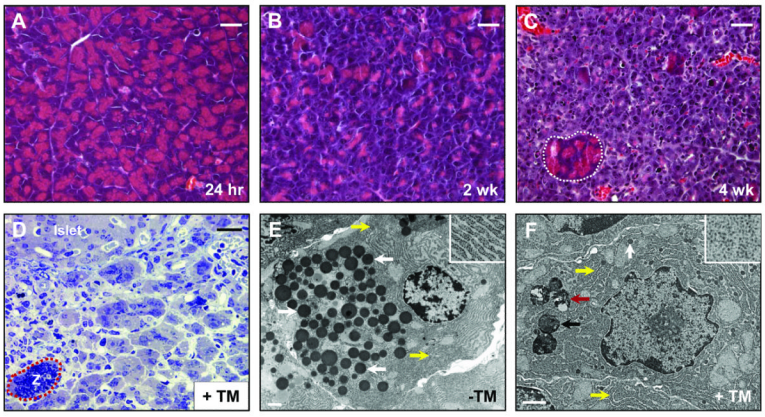

Figure 3. Ablation of Xbp1 leads to severe loss of zymogen granules and alterations in ultrastructure

(A) H&E staining of pancreata 24 hr following Xbp1 ablation. No difference is seen when compared to wild-type pancreata. **(B)** Pancreas 2 wk after Xbp1 ablation. Reduction in eosinic staining across the pancreas is visible, suggesting significant alterations to the zymogen granule compartment. **(C)** Pancreas 4 wk post Xbp1 ablation. Greater than 90% of the exocrine pancreas displays little to no eosinic staining. Rare, isolated regions of acinar-like, ZG-bearing cells remain (white outline). **(D)** Toluidine blue staining of semi-thick sections reveals a completely disrupted exocrine pancreas 4 wk following TM-treatment. Note the rare zymogenic (Z) acinar area (red outline) that remains at this time point. **(E)** Electron micrograph of a control $Xbp1^{fl/fl}$; $Mist1^{CreER/+}$ acinar cell. The extensive accumulation of normal zymogen granules (white arrows) are apically localized. Highly organized rER (yellow arrows and inset) are also visible at the basal edge of the cell. **(F)** Electron micrograph of a typical non-zymogenic acinar cell from 4 wk post TM-treated $Xbp1^{fl/fl}$; $Mist1^{CreER/+}$ mice. Autolysosomes (red arrow), autophagosomes (black arrow), disorganized ER (yellow arrows) and small, abortive zymogen granules (white arrow) can be seen. Inset shows a high mag. image of the extensive free ribosomes found in these cells. Scale = 30 μm (A-D), 1 μm (E-F).

NIH-PA Author Manuscript
NIH-PA Author Manuscript
NIH-PA Author Manuscript

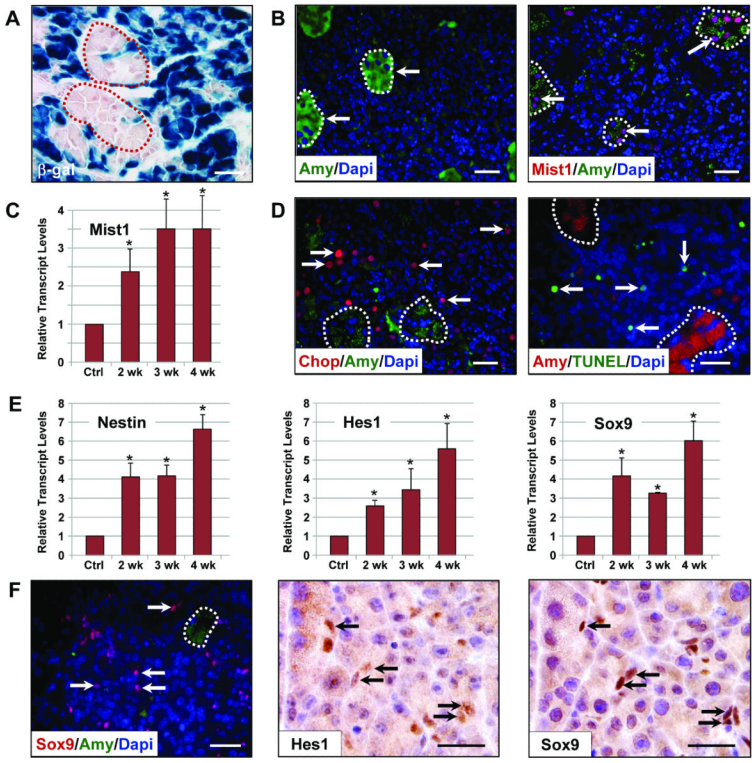

Figure 4. Xbp1$^{\Delta Ex2}$ acinar cells extinguish acinar-specific gene expression and undergo ER stress and programmed cell death

(A) β-gal expression in Xbp1$^{fl/fl}$;Mist1$^{CreER/+}$;R26R^{LacZ} pancreata 4 wk post-TM. The majority of acinar cells are non-zymogenic β-gal positive although isolated, zymogen-containing clusters of acinar cells (outlines) remain β-gal negative. **(B)** Zymogen-containing regions (arrows) accumulate high levels of amylase and MIST1, a transcription factor linked to terminal differentiation of the exocrine pancreas. **(C)** Relative transcript levels of Mist1 reveals an increase in expression following Xbp1 ablation despite restriction to only the zymogenic cell population. **(D)** Localization of the ER stress indicator CHOP and TUNEL-positive cells (arrows) is largely restricted to non-zymogenic cells. Dotted outlines - individual zymogenic-containing acinar units. **(E)** Relative transcript levels of pancreatic progenitor cell genes nestin, Hes1 and Sox9 following Xbp1 ablation. **(F)** Expansion of the centroacinar/terminal duct cell compartment is detected by increased numbers of Hes1 and Sox9 positive cells (arrows) which are amylase negative. Brightfield IHC Hes1, Sox9 - serial sections. Scale = 20 μm. *p<0.05

NIH-PA Author Manuscript

NIH-PA Author Manuscript

NIH-PA Author Manuscript

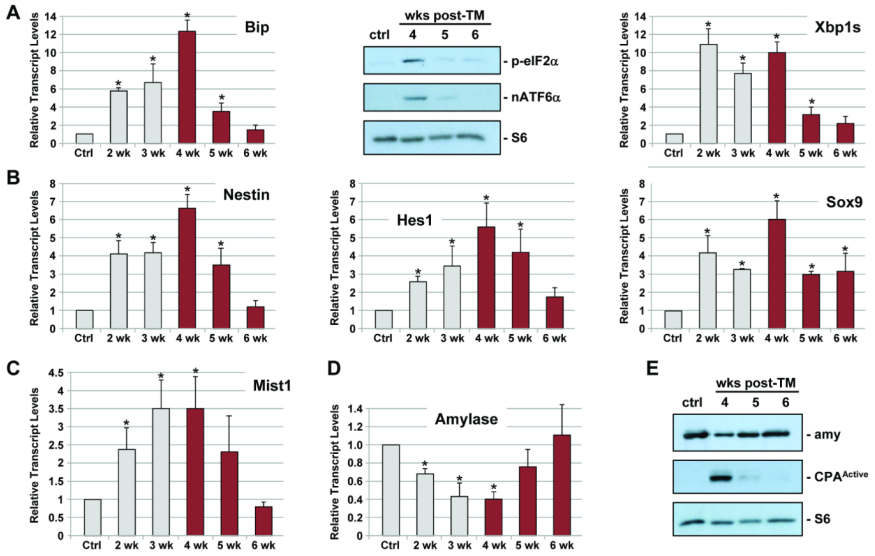

Figure 5. Xbp1$^{\Delta Ex2}$ pancreata undergo a rapid recovery period following peak ER stress and apoptosis responses

(A) Relative transcript and protein levels of the ER stress markers BiP, p-eIF2α, nATF6α and Xbp1s are reduced to near control levels over the 4-6 wk post-TM period. **(B)** Relative transcript levels of pancreatic progenitor cell genes Nestin, Hes1 and Sox9. **(C,D)** Expression of acinar cell terminal differentiation markers Mist1, Amylase and Elastase return to control levels by 6 wk post-TM. **(E)** Amylase and activated CPA (CPA^{Active}) protein levels return to control levels over the duration of the time course. Anti-S6 - loading control. Ctrl - litter mate animals treated with corn oil. *p<0.05

NIH-PA Author Manuscript

NIH-PA Author Manuscript

NIH-PA Author Manuscript

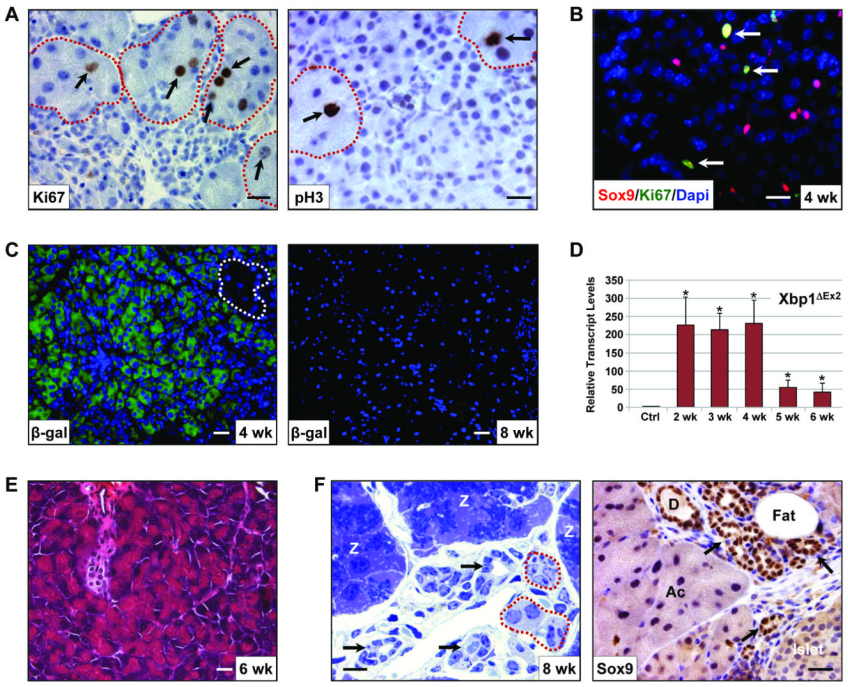

Figure 6. The zymogen-containing subset of acinar cells rapidly proliferates and regenerates the exocrine pancreas

(A) Zymogen-containing populations (red outline) are highly proliferative as evidenced by expression of Ki67 and phospho-histone3 (pH3) (arrows). All non-zymogenic acinar cells remain Ki67 and pH3 negative. **(B)** The Sox9 centroacinar/terminal duct cell compartment is also highly proliferative. **(C)** Anti-β-gal of 4 wk and 8 wk $Xbp1^{\Delta Ex2}$ pancreata showing that the vast majority of acinar cells at 4 wk post-TM are β-gal+. By 8 wk post-TM the exocrine pancreas consists almost entirely of β-gal negative acinar cells. Dotted outline highlights a zymogen-containing acinus. **(D)** $Xbp1^{\Delta Ex2}$ transcript levels over the indicated time points following TM addition. As predicted, replacement of $Xbp1^{\Delta Ex2}$ acinar cells with $Xbp1^{fl/fl}$ acinar cells leads to a loss of the $Xbp1^{\Delta Ex2}$ allele. **(E)** H&E staining reveals the rapid recovery of the acinar cell population by 6 wk post-Xbp1 ablation. **(F)** Toluidine blue staining of semi-thick sections shows the presence of large numbers of zymogen-containing acini (Z) 8 wk post-TM. Zymogen granules are detected as the dark blue staining in the center of the cells. The recovered pancreas also exhibits several other characteristics including the presence of tubular duct-like structures (black arrows), occasional non-zymogenic areas (red outlines) and fat deposition. Note that the tubular complexes are Sox9 positive, suggesting that they are derived from the expanding centroacinar/terminal duct cell compartment. D - duct, Ac - acinar cells. Scale = 20 μm. *p<0.05

NIH-PA Author Manuscript
NIH-PA Author Manuscript
NIH-PA Author Manuscript

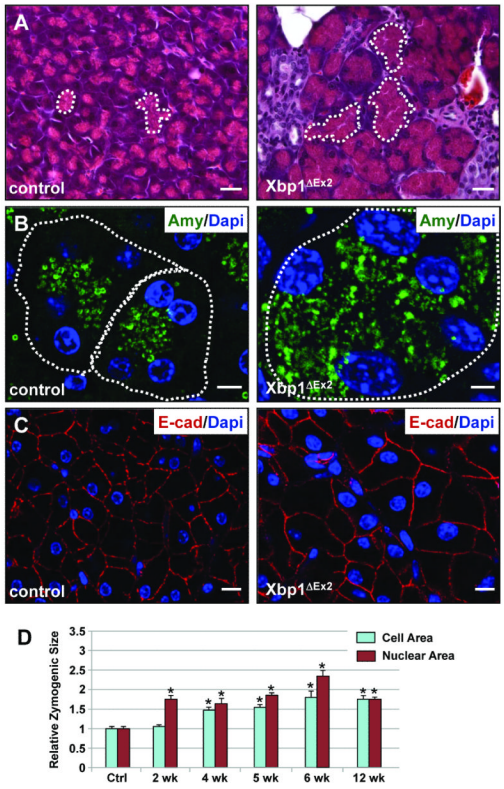

Figure 7. Recovered acini have an expanded zymogen compartment and overall increased cell size relative to control pancreata

(A) Comparison between eosin-stained zymogen compartments in control vs. 12 wk post-ablation pancreata. White dotted lines highlight apically localized zymogens from individual acini. **(B)** Amylase staining in control and 12 wk Xbp1$^{\Delta Ex2}$ pancreata reveal a greatly expanded zymogen compartment in the regenerating acinar cells. Outlines indicate individual acini. **(C)** E-cadherin staining highlights the overall size of individual acinar cells of control and 12 wk post-TM pancreata showing an increased size for the regenerated cells. **(D)** Quantification of nuclear and acinar cell size for control and Xbp1$^{\Delta Ex2}$ pancreata. Scale = 20 μm. *p<0.005